Clin Pharmacokinet (2017) 56:1331–1342
DOI 10.1007/s40262-017-0522-8

ORIGINAL RESEARCH ARTICLE

Population Pharmacokinetic Modeling of JNJ-53718678, a Novel Fusion Inhibitor for the Treatment of Respiratory Syncytial Virus: Results from a Phase I, Double-Blind, Randomized, Placebo-Controlled First-in-Human Study in Healthy Adult Subjects

Dymphy R. H. Huntjens[1] · Sivi Ouwerkerk-Mahadevan[1] · Anne Brochot[1] · Sarah Rusch[2] · Marita Stevens[3] · Rene Verloes[3]

Published online: 25 February 2017

Abstract

Background JNJ-53718678 is a potent small-molecule inhibitor of the F-glycoprotein-mediated complex membrane fusion process of the respiratory syncytial virus. Here, we report the pharmacokinetics, the population pharmacokinetic modeling, and the safety and tolerability of JNJ-53718678 from the first-in-human, double-blind, randomized, placebo-controlled phase I study.

Methods Healthy subjects were randomized (6:3) into five single-dose groups (25–1000 mg) or three multiple-dose groups [250 mg every 24 h (q24h), 500 mg q24h, 250 mg every 12 h; fed conditions for 8 days] to receive JNJ-53718678 or placebo. Blood and urine samples were collected at several timepoints up to 72 h after intake of JNJ-53718678 and analyzed using validated liquid chromatography-mass spectrometry methods. A population pharmacokinetic model was developed and validated.

Results Peak plasma concentrations of JNJ-53718678 increased with increasing single (159 ± 54.9 to 6702 ± 1733 ng/mL) and multiple (on day 8, 1528 ± 256 to 2655 ± 591 ng/mL) doses. Steady-state conditions were reached on day 2 of the 8-day dosing regimen. Less than 4% of JNJ-53718678 was excreted in urine across all dose groups. Mean exposure of JNJ-53718678 was 7% lower in the fed state compared with the fasted state at the same dose. A two-compartment model with first-order absorption with parallel linear and non-linear elimination best described the pharmacokinetics of JNJ-53718678. No covariate effects were observed.

Conclusions A population pharmacokinetic model that describes the concentration data well with good precision of all parameter estimates was developed and validated. JNJ-53718678 was well tolerated at all single and multiple doses studied.

Key Points

The mean maximum plasma concentrations of JNJ-53718678 increased proportionally to increasing single doses (25–1000 mg) of JNJ-53718678, while the mean exposures were slightly more than dose proportional. When repeatedly administered for 8 days, both the mean maximum plasma concentrations and exposures increased proportionally to increasing doses (250–500 mg) of JNJ-53718678.

The mean exposures of JNJ-53718678 were found to be similar before and after a meal and hence JNJ-53718678 may be administered irrespective of food intake.

A robust population pharmacokinetic model that described single- and multiple-dose data in adults was developed. None of the covariate effects altered the pharmacokinetics of JNJ-53718678.

Electronic supplementary material The online version of this article (doi:10.1007/s40262-017-0522-8) contains supplementary material, which is available to authorized users.

✉ Dymphy R. H. Huntjens
DHuntjes@its.jnj.com

[1] Global Clinical Pharmacology, Janssen Pharmaceutica NV, Beerse, Belgium

[2] Statistics and Decision Sciences, Janssen Pharmaceutica NV, Beerse, Belgium

[3] Global Clinical Development, Janssen Pharmaceutica NV, Beerse, Belgium

1 Introduction

Respiratory syncytial virus (RSV) is a negative-stranded ribonucleic acid virus belonging to the Paramyxoviridae family, which also includes the human metapneumovirus and the parainfluenza-virus 3 [1]. The RSV mainly infects the ciliated epithelial cells in the upper respiratory tract exhibiting 'common cold'-like symptoms. This infection may last up to 2–3 weeks and is usually self-limiting. In infants, approximately, 40% of these infections lead to lower respiratory tract infections and are principally characterized by bronchiolitis and pneumonia [2, 3].

In 2005, globally, 33.8 million new cases of RSV-associated acute lower respiratory tract infections were reported in children younger than 5 years of age (22% of total acute lower respiratory tract infections globally). Of these, 3.4 million needed hospitalization and up to 0.2 million children died [4]. According to the Centers for Disease Control and Prevention, RSV is the most common cause of bronchiolitis at 2 years of age [2, 3, 5]. In addition, RSV infection results in substantial illness and morbidity in the elderly and adults with underlying chronic illnesses, underlying disorders of cellular immunity, or suppressed immune systems [6].

Current treatment options for the management of bronchiolitis and pneumonia are driven by evidence-based guidelines such as the American Academy of Pediatrics guideline 2014, Royal Australian College of General Practitioners 2008, Scottish Intercollegiate Guidelines Network 2006, and the National Institute for Health and Care Excellence 2015. Treatments may be categorized as supportive (majorly supplemental oxygen, nebulized hypertonic saline or nasal saline drops, nasogastric or intravenous fluids for hydration, nasal suction for respiratory distress), prophylactic (immunoprophylaxis with the humanized monoclonal antibody palivizumab), and therapeutic (inhaled ribavirin, no longer recommended by the American Academy of Pediatrics) [2]. Thus, there is an unmet medical need prophylactically (pre- and post-exposure) and therapeutically in both children and adults.

After exposure to the virus, clinical symptoms appear on day 3 but the peak viral load is on day 6, increasing the likelihood that direct antivirals (small molecules or biologicals) can be viable RSV treatments and achieve high and sustained antiviral responses and improve disease outcome [7].

Enveloped viruses such as RSV have complex membrane fusion machinery. The RSV has two surface proteins, G and F (fusion glycoprotein) that bring about binding and fusion, respectively. Upon fusion to the host cell membrane, the viral nucleic acid is deposited into the host cells and its replication is initiated [2, 8]. JNJ-53718678, a small-molecule (indole class) RSV-specific fusion inhibitor, inhibits this F-glycoprotein-mediated complex membrane fusion process and is thus being developed for the treatment of respiratory tract diseases caused by human RSV [9, 10].

The objectives of this phase I study were to (1) investigate the pharmacokinetics of JNJ-53718678 after single or multiple (for 8 days) oral doses, (2) assess the food effect at a single-dose level, and (3) assess the safety and tolerability of JNJ-53718678. Based on the pharmacokinetic (PK) data, an exploratory analysis was conducted to develop a population PK model for JNJ-53718678.

2 Methods

2.1 Study Design and Drug Administration

This was a first-in-human, double-blind, randomized, placebo-controlled phase I study in healthy adult subjects (EudraCT Number: 2014-001848-37). The selection of the doses was based on the no observed adverse effect levels from the animal toxicity studies, in particular, the most sensitive species having the lowest no observed adverse effect level, conversion to human equivalent doses, and the application of a safety factor of 10 or more for the starting dose.

For the single-dose escalation (SDE) part of the study, subjects were enrolled into one of the two SDE panels. One SDE panel had three dose groups while the other had two dose groups. Subjects in each SDE panel were randomized to receive either JNJ-53718678 (six subjects) or placebo (three subjects) under fasted conditions. Thus, subjects who received JNJ-53718678 in one treatment may have received placebo in the subsequent treatment and vice-versa. A washout period of at least 10 days between subsequent intakes of the study drug was maintained. Food effect was studied by comparing the PK data of subjects who received a single dose of 250 mg JNJ-53718678 under fasted and fed conditions.

For the multiple-dose escalation (MDE) part of the study, successive panels of nine subjects each received either JNJ-53718678 (six subjects) at a dose of 250 mg every 24 h (q24h), 500 mg q24h, or 250 mg every 12 h (q12h) or placebo (three subjects each), under fed conditions for 8 days. Subjects were administered a 20-mg/mL oral solution of JNJ-53718678 (base) in a vehicle consisting of hydroxyl-propyl-β-cyclodextrin, sodium hydroxide, concentrated hydrochloride acid, and purified water, or the vehicle alone (placebo group). Formulation limitations restricted the doses to 1000 mg in the SDE panels and 500 mg q24h in the MDE panels of the study.

Doses were escalated after JNJ-53718678 was determined to be safe, well tolerated, and the maximum tolerated dose not reached from 72-h safety and 24-h PK data. Additionally, doses were to be escalated only if the

expected maximum plasma concentration (C_{max}) or area under the curve from time zero to 24 h (AUC_{24h}) did not exceed 9 or 100 μg·h/mL, respectively. These ceiling values were derived from exposure outcomes of JNJ-53718678 in well-tolerated non-clinical toxicity studies, including a cardiovascular toxicity study in dogs.

No formal sample size determination and power calculations have been performed for this study because no clinical data were available for JNJ-53718678. A standard design was applied and nine subjects (six on active and three on placebo) were included in every dose group.

2.2 Subject Selection and Eligibility

Male or female adult (≥18 and ≤55 years of age) subjects with a body mass index of ≥18 and ≤30 kg/m^2 were enrolled. Subjects were required to be healthy and normal at the physical examination, medical history, vital signs, electrocardiogram (ECG), and laboratory tests performed at screening. Women were to be of non-childbearing potential (post-menopausal for at least 2 years or surgically sterile or incapable of becoming pregnant), negative for pregnancy at screening, and not breastfeeding. Subjects were to be excluded in the case of any history of cardiac arrhythmias, prolonged corrected QT interval (>450 ms), or risk factors for torsade de pointes syndrome such as hypokalemia or a family history of long QT syndrome. Other exclusion criteria were a history of drug allergy (including experimental drugs), hepatitis A, B, or C, human immunodeficiency virus-1 or -2 infections at screening, history or evidence of use of alcohol, barbiturates, amphetamines, or recreational or narcotic drug use within 1 year before screening.

2.3 Pharmacokinetic Sampling

Blood samples were collected for the measurement of plasma concentrations of JNJ-53718678 at pre-dose, 0.5, 1.0, 1.5, 2.0, 3.0, 4.0, 6.0, 8.0, 12.0, 16.0, 24.0, 36.0, 48.0, and 72.0 h after single and multiple dosing (days 1 and 8). For all multiple-dosing groups, only pre-dose blood samples were collected on days 2–7. For the q24h groups, blood was collected at an additional timepoint of 14.0 h on day 1. Full urinary output was collected at multiple time intervals up to 72 h after intake of the study drug.

2.4 Analytical Methods

2.4.1 Plasma Samples

Plasma was separated by protein precipitation and then analyzed to determine JNJ-53718678 concentrations using a validated, specific, and sensitive liquid chromatography-tandem mass spectrometry method. The Shimadzu LC20AD or LC30AD (Shimadzu Scientific instruments, Columbia, USA) liquid chromatograph (high-performance liquid chromatography mode) with a 3.5-μm XBridge C18 column coupled with the API-4000 LC-MS/MS system (Applied Biosystems/MDS SCIEX, Foster City, USA) was used to analyze the plasma samples. Twenty-five microliters of calibration, quality control, and study samples were diluted with blank human di-potassium ethylenediaminetetraacetic acid plasma and methanol and extracted with acetonitrile prior to analysis. The calibration curve contained at least six non-zero calibration standards. Linearity was established by back-calculated values of calibration samples. The acceptance criteria for precision and accuracy were set at ≤15.0% coefficient of variation (CV) and within ±15.0% bias, respectively, except for the lower limit of quantification (LLOQ) where the bias had to be within ±20.0% of the nominal value. The LLOQ was 1.0 ng/mL.

2.4.2 Urine Samples

Urine samples were also processed in the same manner as plasma samples, substituting blank human urine plus 0.2% Tween for blank human di-potassium ethylenediaminetetraacetic acid plasma. The calibration curve comprised at least six non-zero calibration standards. The linearity was established by back-calculated values of calibration samples. The acceptance criteria for precision and accuracy were set at ≤20.0% CV and within ±20.0% bias, respectively, except for the LLOQ where the bias had to be within ±25.0% of the nominal value. The LLOQ was 10 ng/mL.

2.5 Pharmacokinetic Analysis and Statistics

2.5.1 Non-compartmental Analysis

Plasma and urine PK parameters were derived for JNJ-53718678. A non-compartmental analysis of the PK parameters was performed using Phoenix™ WinNonlin® (Version 6.2.1, Certara, Princeton NJ, USA). Descriptive statistics were calculated for plasma concentrations at each timepoint and for the derived plasma and urine PK parameters.

2.5.2 Population Pharmacokinetic Modeling

Population PK modeling was conducted with NONMEM (Version 7.2; ICON plc, Dublin, Ireland) in conjunction with a gfortan (64-bit) compiler using Perl-Speaks NONMEM (Version 3.5.3, PSN) [11] and R (Version 3.2), while XPOSE4 and R were used for diagnostic plots. Four samples, identified as outliers [conditional weighted residuals (CWRES) >6] were excluded from the dataset. The final dataset contained 36 subjects and 1034 PK samples.

2.5.2.1 Structural Model Development The first-order conditional estimation with interaction method in NONMEM was used for model development. Log-transformed plasma concentration-time data were evaluated using various compartmental models. The zero- and first-order absorption, linear clearance, and Michaelis–Menten elimination and distribution models were tested and their results compared. Inter-individual variability was described using an exponential model. The residual error for log-transformed JNJ-53718678 plasma concentrations was modeled using an additive error model. ADVAN13 was used for the final model (Model code in Online Resource 1). Thirty samples of below the limit of quantification, (<3%) were omitted during model development.

The final selection of the structural model was based on goodness-of-fit plots, the comparison of nested models [based on the reduction in minimum objective function value (OBJ) of $\geq$6.63 ($p < 0.01$)], the precision of the estimated parameters, and the decrease in the residual error variance. After determination of the base structural model, the contributions of continuous and categorical covariates such as age, body weight, and creatinine clearance to the population parameter variability were assessed. Food status was directly included in the base model as food effect on absorption was necessary to obtain proper minimization.

The precision of parameter estimates and stability of the final population PK model were evaluated using a bootstrap procedure (1000 replications). The median and standard deviation of the bootstrap results were determined and compared with the final model population values. Prediction-corrected visual predictive checks were used to characterize the predictive performance of the final model, as this technique is more informative than a traditional visual predictive check binned by the different designs of the phase I trial given the limited amount of data per bin [12]. The parameter estimates, population parameter variability, and residual unexplained variability were used to generate 1000 simulated datasets from which median and 90% prediction intervals (5th–95th percentiles) of the simulated values were determined and compared with observed values. Runs that did not minimize successfully were excluded from the analysis.

2.6 Metabolism

JNJ-53718678 is known to be metabolized in vitro by cytochrome P450 (CYP) 3A4 in human microsomes. In addition, JNJ-53718678 is a moderate-to-strong inhibitor of CYP3A4 (IC_{50}: 1–2 μM, data on file) as well as an inducer of CYP3A4 in human hepatocytes at $\geq$1.5 μM. 4β-Hydroxycholesterol is a known endogenous marker of CYP3A induction [13]. Hence, 4β-hydroxycholesterol was measured in plasma samples in the MDE panel at baseline (pre-dose on day 1) and at 4 h post-dose on days' 1 and 8 to assess CYP3A activity.

2.7 Safety Evaluation

Safety and tolerability were evaluated throughout the study. All clinically relevant changes were recorded as adverse events (AEs) and graded in accordance with the World Health Organization's Toxicity Grading Scale for determining the severity of AEs, February 2003 [14]. Other safety evaluations: including hematology, serum chemistry, urinalysis, occult blood in feces, ECGs, and vital signs were recorded at screening and at subsequent pre-specified timepoints throughout the study.

3 Results and Conclusions

3.1 Study Population

Forty-five subjects were enrolled into two SDE panels and three MDE panels, as planned. In each panel, subjects were randomized to receive either JNJ-53718678 (six subjects) or placebo (three subjects) (Fig. 1). All subjects except one (SDE panel; planned to receive placebo in the next treatment; ongoing AE: gastroenteritis) were treated as planned and completed the study.

The demographic characteristics were similar between the two SDE panels (Table 1). In the MDE panels, except for sex inequality (majority were male), the other demographic characteristics were comparable. All subjects tested negative for hepatitis A, B, and C, human immunodeficiency virus-1 and -2, drug use, and alcohol breath.

3.2 Pharmacokinetics

3.2.1 Single-Dose Pharmacokinetics in Plasma

Under fasted conditions, with increasing single doses of JNJ-53718678 from 25 to 1000 mg, the increase in mean C_{max} was dose proportional and the increase in mean area under the curve from time zero to infinity (AUC_{∞}) was slightly more than dose proportional. The median time to reach maximum plasma concentration (t_{max}) was 1.0 h at all doses except 1000 mg (2.5 h) (Table 2; Fig. 2).

3.2.2 Effect of Food on Single-Dose Pharmacokinetics in Plasma

Under fed conditions, the mean C_{max} of JNJ-53718678 was approximately 35% lower than under fasted conditions (1.20 vs. 1.97 μg/mL), whereas the mean AUC_{∞} was only 7% lower under fed conditions. The median t_{max} was

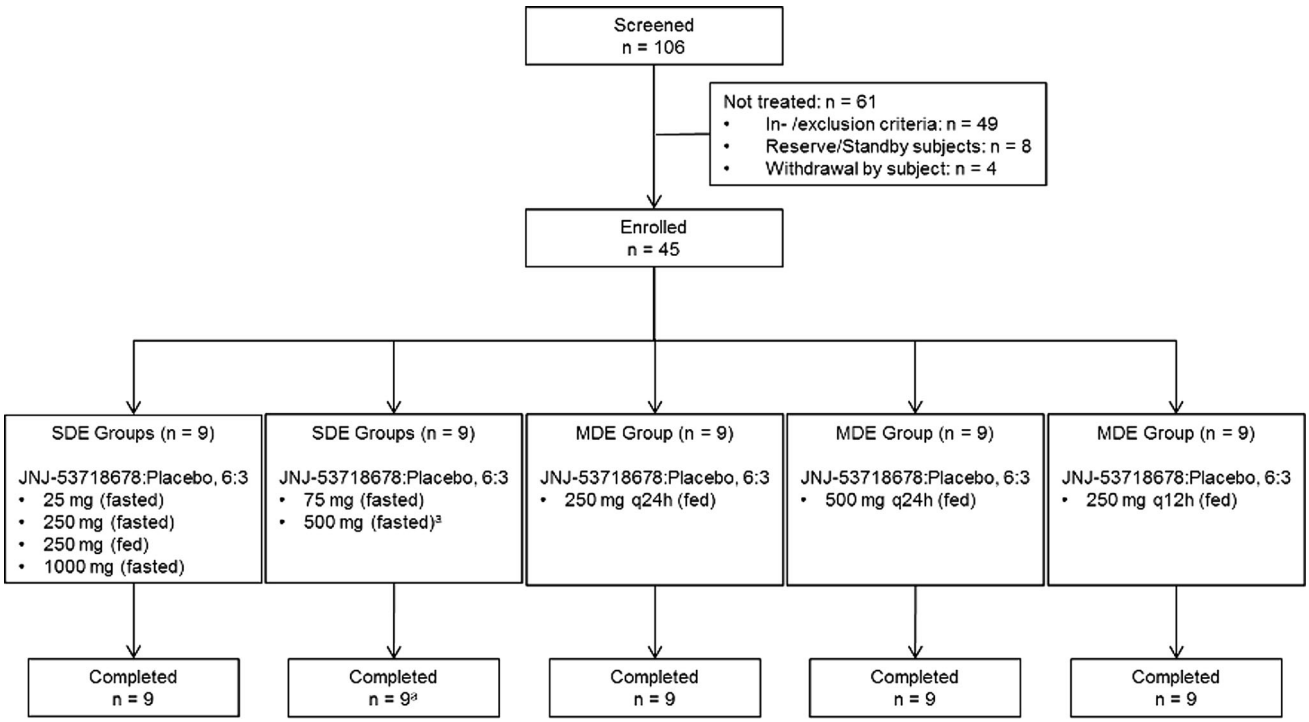

Fig. 1 Subject disposition. [a]One subject received 75 mg of JNJ-53718678 in session II and was randomized to the placebo group in session IV and did not receive study treatment in that session because of an ongoing adverse event of gastroenteritis, which started during the follow-up period of session II and was considered by the investigator to be not related to the study drug. However, as this subject completed the assessments of the last study visit, per protocol, this subject was considered to have completed the study. *MDE* multiple-dose escalation, *n* number of subjects, *q12h/24h* every 12 h/24 h, *SDE* single-dose escalation

Table 1 Demographic data for subjects across dose groups in the study (intent-to-treat population)

	SDE groups		MDE groups		
	JNJ-53718678 25, 250, and 1000 mg or placebo ($N = 9$)	JNJ-53718678 75 and 500 mg or placebo ($N = 9$)	JNJ-53718678 250 mg q24h or placebo ($N = 9$)	JNJ-53718678 500 mg q24h or placebo ($N = 9$)	JNJ-53718678 250 mg q12h or placebo ($N = 9$)
Age (years)					
Median (range)	50.0 (33–55)	50.0 (25–55)	44.0 (22–55)	41.0 (30–55)	47.0 (36–53)
Sex, *n* (%)					
Female	5 (55.6)	5 (55.6)	2 (22.2)	3 (33.3)	1 (11.1)
Male	4 (44.4)	4 (44.4)	7 (77.8)	6 (66.7)	8 (88.9)
Baseline BMI (kg/m^2)					
Median (range)	24.60 (18.3–27.3)	24.60 (18.5–26.8)	23.00 (21.7–29.0)	24.40 (23.3–27.4)	26.00 (22.4–28.8)

BMI body mass index, *MDE* multiple-dose escalation, *N* number of subjects in the intent-to-treat population, *n* number of subjects within each sex, *q12h/24h* every 12 h/24 h, *SDE* single-dose escalation

reached later under fed conditions (3.5 h) than under fasted conditions (1.0 h) (Fig. 3).

3.2.3 Multiple-Dose Pharmacokinetics in Plasma

The mean C_{max} and AUC_{24h} values on days 1 and 8 (at steady state) increased proportionally when the dose was increased from 250 mg q24h to 500 mg q24h (Table 3; Fig. 4). The mean trough concentrations (C_{trough}) were similar within each dose panel from day 2 through day 8, indicating that steady state was reached on day 2. Compared with day 1, the mean C_{max} and AUC_{24h} values increased on day 8 in the 250 mg q24h (by 1.20- and 1.26-fold, respectively) and 500 mg q24h (by 1.15- and 1.16-fold, respectively) panels. Similarly, the mean C_{max} and area under the curve from time zero to 12 h (AUC_{12h}) values also increased on day 8 (by 1.42- and 1.53-fold, respectively) in the 250 mg q12h panel.

Table 2 Pharmacokinetics of JNJ-53718678 in plasma after single-dose administration of JNJ-53718678 (fasted conditions)

	Mean ± standard deviation, t_{max}: median (range)				
	25 mg (n = 6)	75 mg (n = 6)	250 mg (n = 6)	500 mg (n = 6)	1000 mg (n = 6)
$C_{max,}$ ng/mL	159 ± 54.9	497 ± 67.9	1967 ± 772	3555 ± 568	6702 ± 1733
$t_{max,}$ h	1.00 (0.50–1.01)	1.00 (1.00–1.50)	1.00 (0.50–1.50)	0.99 (0.99–3.01)	2.50 (1.00–4.03)
$AUC_{\infty,}$ ng·h/mL	988 ± 481	3558 ± 919	15,379 ± 6505	32,861 ± 4660	72,773 ± 13,870
$t_{1/2term,}$ h	6.6 ± 2.1	10.3 ± 2.4	9.3 ± 2.8	9.6 ± 1.0	9.3 ± 1.1
CL/F, L/h	30.1 ± 12.7	22.0 ± 4.45	18.9 ± 7.98	15.5 ± 1.99	14.2 ± 2.65
V_d/F, L	259 ± 58.4	327 ± 107	240 ± 88.9	213 ± 24.7	189 ± 34.5

AUC_∞ area under the curve from time zero to infinity, *C_{max}* maximum plasma concentration, *CL/F* total apparent oral clearance, *n* number of subjects with pharmacokinetic data, *$t_{1/2term}$* terminal half-life, *t_{max}* time to reach maximum plasma concentration, *V_d/F* apparent volume of distribution

$AUC_{0–last}$ is similar to AUC_∞, as for all individuals the percent extrapolated was <3%

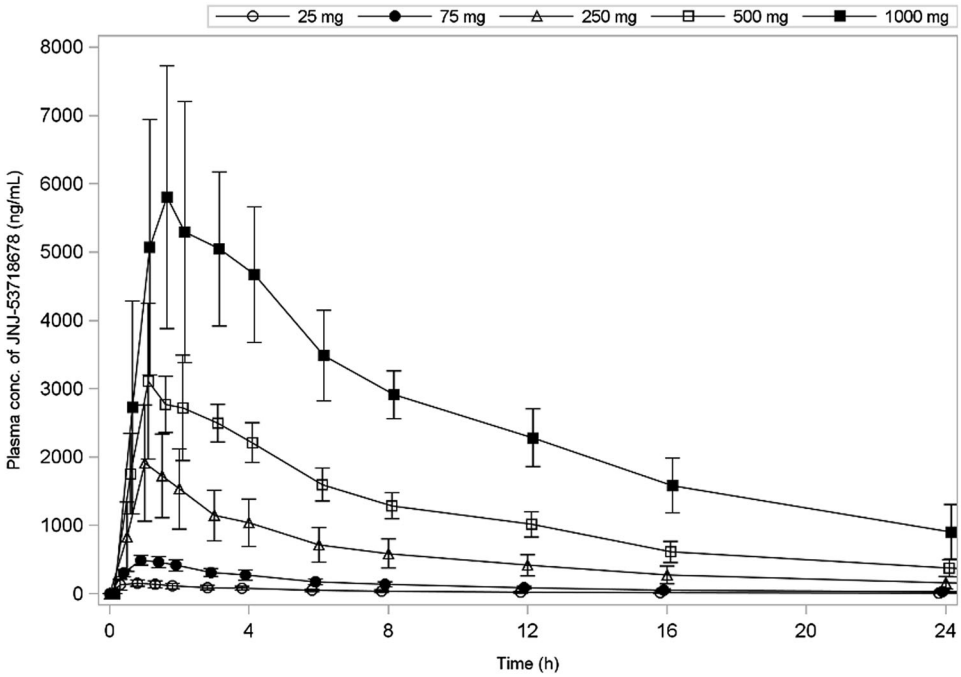

Fig. 2 Mean (±standard deviation) plasma concentration-time curves of JNJ-53718678 after administration of a single dose of JNJ-53718678 at 25, 75, 250, 500, and 1000 mg under fasted conditions. *conc.* concentration

3.2.4 *Effect of Dosing Regimen on Pharmacokinetics of JNJ-53718678*

The day 8 mean dose-normalized C_{max} and C_{trough} values were lower for the 500 mg q24h panel compared with the 250 mg q12h panel (5.31 ± 1.18 vs. 6.55 ± 1.23 ng/mL/mg and 1.12 ± 1.11 vs. 2.69 ± 0.66 ng/mL/mg), whereas the exposure (AUC_{24h}) values were slightly higher for the 500 mg q24h panel compared with the 250 mg q12h panel (62.3 ± 25.4 vs. 50.9 ± 10.5 ng·h/mL/mg).

3.2.5 *Urine Pharmacokinetics in the Single- and Multiple-Dose Panels*

The mean percentage of JNJ-53718678 excreted in urine and its renal clearance was low and comparable between the 500 mg q24h and 250 mg q12h panels (Table 4). As the mean percentage excretion of JNJ-53718678 in urine is low, it may be concluded that clearance via the renal pathway is minor.

3.2.6 *Population Pharmacokinetic Model Development and Validation*

A two-compartment model with first-order absorption and a parallel linear and a non-linear elimination pathway best described the JNJ-53718678 data. The model parameters were apparent clearance (CL/F), apparent volume of the central (V_c/F) and peripheral (V_p/F) compartments, apparent inter-compartmental clearance, first-order absorption rate constant (Ka), maximum elimination rate (V_{max}), and Michaelis–Menten constant (K_m, drug concentration at

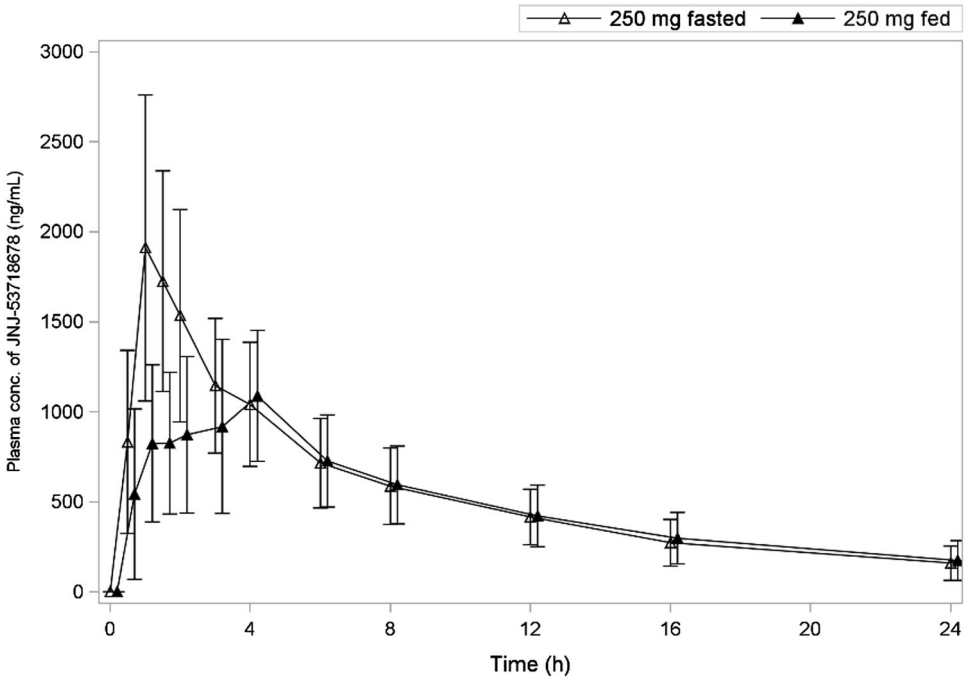

Fig. 3 Mean (±standard deviation) plasma concentration-time curves of JNJ-53718678 after administration of a single dose of JNJ-53718678 at 250 mg under fasted conditions and under fed conditions. *conc.* concentration

Table 3 Pharmacokinetics of JNJ-53718678 in plasma after multiple-dose administration of JNJ-53718678 (fed conditions)

	Mean ± standard deviation, t_{max}: median (range)		
	250 mg q24h ($n = 6$)	500 mg q24h ($n = 6$)	250 mg q12h ($n = 6$)
Day 1			
$C_{max,}$ ng/mL	1273 ± 150	2322 ± 336	1167 ± 206
$t_{max,}$ h	1.75 (1.00–4.02)	3.00 (2.00–4.00)	3.00 (1.01–4.00)
$AUC_{12h,}$ ng·h/mL			8494 ± 1886
$AUC_{24h,}$ ng·h/mL	13,886 ± 3147	26,684 ± 6885	16,988[a] ± 3772
Day 8			
$C_{max,}$ ng/mL	1528 ± 256	2655 ± 591	1637 ± 308
$C_{trough,}$ ng/mL	313 ± 224	558 ± 553	672 ± 165
$t_{max,}$ h	2.00 (1.00–4.01)	3.01 (1.50–4.03)	1.75 (1.00–4.00)
$t_{1/2term,}$ h	11.5 ± 2.1	9.5 ± 2.6	9.4 ± 1.2
$AUC_{12h,}$ ng·h/mL			12,719 ± 2619
$AUC_{24h,}$ ng·h/mL	17,805 ± 6158	31,165 ± 12686	25,438[a] ± 5238
CL/*F*, L/h	15.2 ± 4.10	17.8 ± 5.56	20.3 ± 3.79

AUC_{12h} area under the curve from time zero to 12 h, *AUC_{24h}* area under the curve from time zero to 24 h, *C_{max}* maximum plasma concentration, *C_{trough}* mean trough concentration, *CL/F* total apparent oral clearance, *n* number of subjects with pharmacokinetic data, *q12h/24h* every 12 h/24 h, *t1/2term* terminal half-life, *t_{max}* time to reach maximum plasma concentration

[a] AUC_{24h} was calculated as $2 \times AUC_{12h}$

50% V_{max}). The final population PK parameters estimates are provided in Table 5. The relative standard errors of parameter estimates ranged from 3.1 to 29.5%.

Intake of food was a significant covariate on Ka (−107 OBJ points). Between-subject variability could be identified on Ka, CL/*F*, V_{max}, V_c/F, and V_p/F. Only body weight was a significant covariate on V_c/F (−14 OBJ points); however, the coefficient of variation (%CV) on K_m became unacceptably large (>8900%) and therefore, it was not retained in the final model. There was no significant drop in OBJ with the addition of creatinine clearance on CL/*F* or V_{max}. The median parameter values resulting from the bootstrap procedure agreed with the estimates from the final population model. This suggests that the parameters in the final model were reasonably well determined and the model was stable. From 1000 bootstrap runs, 728 were

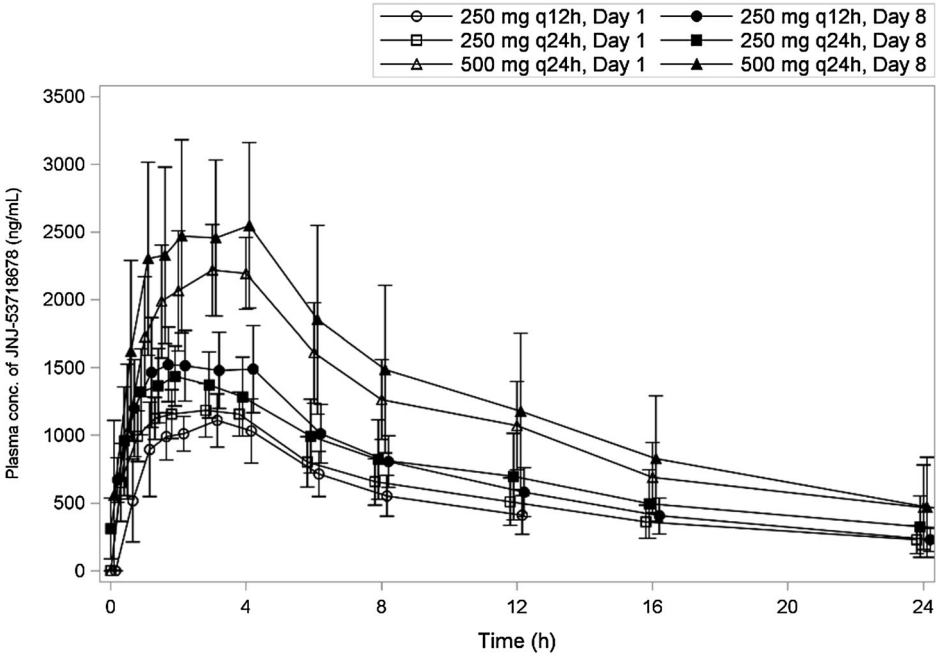

Fig. 4 Mean (±standard deviation) plasma concentration-time curves of JNJ-53718678 after administration of JNJ-53718678 at 250 mg q24h, 500 mg q24h, or 250 mg q12h under fed conditions on days 1 and 8

Table 4 Pharmacokinetics of JNJ-53718678 in urine after single- and multiple-dose administrations of JNJ-53718678 (fasted and fed conditions)

	Mean ± standard deviation [%CV]				
	SDE groups (fasted)		MDE groups (fed)		
	250 mg ($n = 4$)	500 mg ($n = 6$)	250 mg q24h ($n = 6$)	500 mg q24h ($n = 6$)	250 mg q12h ($n = 6$)[c]
Ae[a], mg	5.05 ± 1.61 [32.0]	5.78 ± 2.88 [49.9]	9.34 ± 6.28 [67.2]	9.43 ± 6.04 [64.0]	4.40 ± 2.72 [61.8]
D_{urine}[b], %	2.02 ± 0.65 [32.0]	1.16 ± 0.58 [49.9]	3.74 ± 2.51 [67.2]	1.89 ± 1.21 [64.0]	1.76 ± 1.09 [61.8]
CL_R, L/h	0.31 ± 0.07 [21.8]	0.18 ± 0.10 [57.0]	0.54 ± 0.35 [64.4]	0.33 ± 0.19 [58.6]	0.36 ± 0.25 [70.8]

Ae total amount excreted in the urine, CL_R renal clearance, *%CV* percent coefficient of variation, D_{urine} total percentage of the dose excreted in urine, *MDE* multiple-dose escalation, *n* number of subjects, *q12h/24h* every 12 h/24 h, *SDE* single-dose escalation

[a] Ae is $Ae_{0–72}$ for single-dose administration groups, $Ae_{0–24}$ for the q24h multiple-dose administration groups, and $Ae_{0–12}$ for the q12h multiple-dose administration group

[b] D_{urine} is $D_{urine,0–72}$ for single-dose administration groups, $D_{urine,0–24}$ for the q24h multiple-dose administration groups, and $D_{urine,0–12}$ for the q12h multiple-dose administration group

[c] Only a morning dose was administered on day 8

minimized successfully and included in the bootstrap analysis, the results of which are summarized in Table 5.

From the prediction-corrected visual predictive checks, the model performance was considered appropriate for its predictive performance and robust enough for extrapolation (Fig. 5). The plot shows that most of the observed concentrations on all dose levels fell within the 2.5th–97.5th percentile prediction interval. Less than 10% of the observed concentrations lay outside of the prediction intervals. The prediction-corrected visual predictive check shows that the final model adequately describes the majority of the data. The diagnostic plots of individual and population-predicted concentrations vs. observed concentrations were symmetrically distributed around the line of unity and no trends were observed in the CWRES diagnostic plots, indicating that the model adequately describes the JNJ-53718678 PK profile (Online Resources 2 and 3).

3.3 Metabolism

The mean baseline corrected 4β-hydroxycholesterol concentrations were similar between the 250 mg q24h group and placebo on day 1 (1.13 ± 1.42 vs. 0.50 ± 2.08 ng/mL) and day 8 (2.75 ± 5.38 vs. 1.53 ± 1.20 ng/mL). These mean baseline corrected concentrations were also similar between the 500 mg q24h group (0.90 ± 1.66 ng/mL), the 250 mg q12h group (2.40 ± 1.47 ng/mL), and placebo on day 1 (0.50 ± 2.08 ng/mL). On day 8, the mean baseline

Table 5 Parameter estimates and results of the bootstrap runs of the final population PK model

Parameters	Parameter estimate [SE (CV%)]	Bootstrap (n = 728 of 1000 runs were successful)		
		Median	95% CI (lower limit)	95% CI (upper limit)
Fixed				
Ka_{fasted} (1/h)	2.3 (6.8)	2.3	1.9	2.8
Ka_{fed} (1/h)	0.96 (3.1)	1.0	0.7	1.3
CL/*F* (L/h)	12.3 (8.6)	12.3	9.6	14.8
K_m (ng/L)	757 (17.6)	756	487	1287
V_{max} (ng/h)	7.25 (29.5)	7.2	2.9	15.9
V_c/F (L)	164 (3.3)	164	149	178
Q/*F* (L/h)	4.8 (7.0)	4.8	3.1	8.0
V_p/F	47.5 (3.6)	47.4	34.6	63.7
Random effect				
Ka_{fasted} (1/h)	39.8 (20.7)	37.8	19.6	53.0
Ka_{fed} (1/h)	54.9 (18.6)	53.6	31.2	76.1
CL/*F* (L/h)	27.7 (16.2)	27.0	18.0	35.1
V_{max} (ng/h)	60.4 (17.0)	58.2	38.0	90.9
V_c/F (L)	17.9 (14.3)	17.7	12.2	22.2
V_p/F (L)	17.9 (18.6)	17.4	9.5	25.7
Residual error				
Proportional error (%)	18.7 (5.4)	18.6	16.6	20.7
Shrinkage				
Ka_{fasted} (CV%)	44.2			
Ka_{fed} (CV%)	23.7			
CL/*F* (CV%)	14.9			
V_{max} (CV%)	18.5			
V_c/F (CV%)	7.9			
V_p/F (CV%)	20.3			
Proportional error (%)	6.6			

BSV between-subject variability, *CI* confidence interval, *CL/F* apparent clearance, *%CV* percent coefficient of variation, *Kafasted* first-order absorption rate constant for fasted subjects, *Kafed* first-order absorption rate constant for fed subjects, *Km* Michaelis–Menten constant, *n* number of successful bootstrap runs of the total of 100 run, V_{max} maximum metabolic rate, *Vc/F* central volume of distribution, *Vp/F* peripheral volume of distribution, *Q/F* apparent inter-compartmental clearance, *SE* standard error estimate

corrected concentrations were higher for the 500 mg q24h group (7.92 ± 3.41 ng/mL) and the 250 mg q12h group (13.0 ± 5.61 ng/mL) compared with the placebo group (1.53 ± 1.20 ng/mL). This indicated an induction of CYP3A by JNJ-53718678 on day 8 at 500 mg q24h and a relatively higher induction by 250 mg q12h dosing regimens.

3.4 Safety

The most frequent treatment-emergent AEs (TEAEs) at ≥15% incidence in either of the JNJ-53718678 groups are presented in Table 6. No deaths or serious TEAEs were reported. Only one subject, from the SDE panel who received 75 mg JNJ-53718678 and was randomized to receive placebo subsequently, did not receive placebo (permanently discontinued JNJ-53718678) because of ongoing gastroenteritis assessed by the investigator to be unrelated to JNJ-53718678.

Amongst the SDE panels, 94.4% of the subjects experienced at least one TEAE on JNJ-53718678 compared with 42.9% on placebo. All but one (placebo group, Grade 3 headache) of the reported TEAEs and graded laboratory abnormalities were either Grade 1 or 2 in severity. The most frequent TEAEs (≥15%) in subjects on JNJ-53718678, compared with placebo, were dysgeusia (55.6 vs. 0%), headache (22.2 vs. 21.4%), abdominal discomfort (22.2 vs. 0%), back pain (16.7 vs. 7.1%), and hypercholesterolemia (16.7 vs. 0%). Dysgeusia was the most frequent TEAE assessed by the investigator to be at least possibly related to JNJ-53718678.

Amongst the MDE groups, 72.2% of the subjects experienced at least one TEAE on JNJ-53718678 compared with 66.7% on placebo. All the reported TEAEs and graded

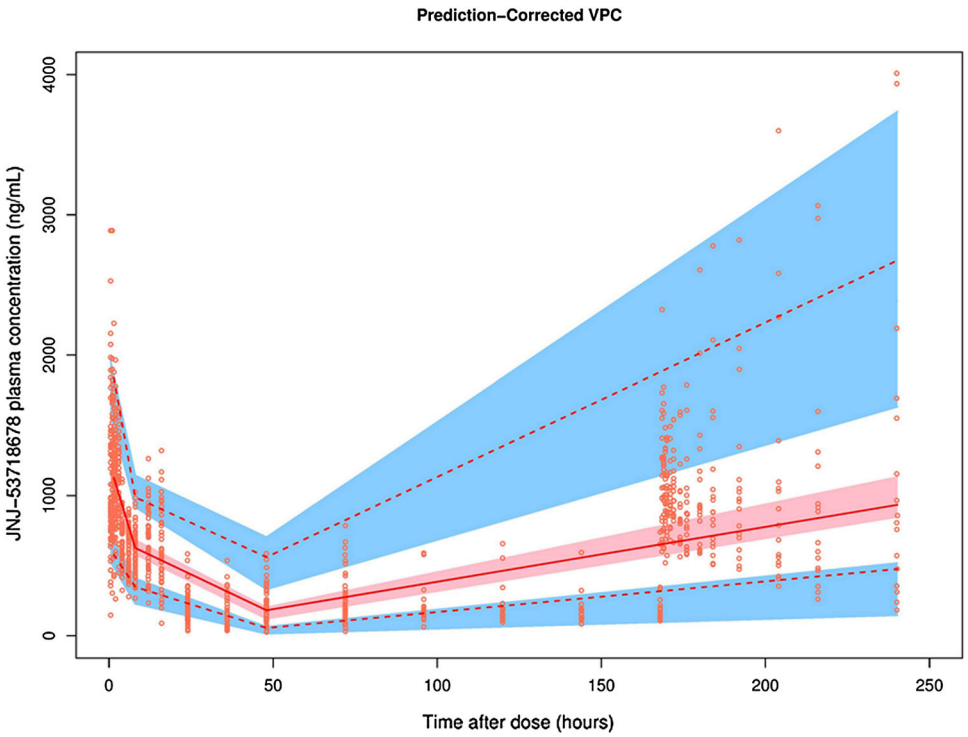

Fig. 5 Prediction-corrected visual predictive check (VPC) plot examines the model's predictive performance. The *solid red line* represents the median observed prediction-corrected plasma concentration (ng/mL) and the *semitransparent red field* represents a simulation-based 95% confidence interval for the median. The observed 5 and 95% percentiles are presented with *dashed red lines*, and the 95% confidence intervals for the corresponding model-predicted percentiles are shown as *semitransparent blue fields*. The observed prediction-corrected plasma concentrations are represented by *red circles*. The plot shows that most of the observed concentrations on all dose levels fell within the 2.5th–97.5th percentile prediction interval

Table 6 Most frequent treatment-emergent adverse events (TEAEs) at ≥15% incidence in either of the JNJ-53718678 groups during the study

	SDE groups		MDE groups	
	JNJ-53718678 ($N = 18$)	Placebo ($N = 14$)	JNJ-53718678 ($N = 18$)	Placebo ($N = 9$)
Any TEAE, *n* (%)	17 (94.4)	6 (42.9)	13 (72.2)	6 (66.7)
Body system or organ class/dictionary-derived term, *n* (%)				
Nervous system disorders	13 (72.2)	3 (21.4)	6 (33.3)	0
Dysgeusia	10 (55.6)	0	3 (16.7)	0
Headache	4 (22.2)	3 (21.4)	2 (11.1)	0
Gastrointestinal disorders	7 (38.9)	2 (14.3)	4 (22.2)	1 (11.1)
Abdominal discomfort	4 (22.2)	0		
Musculoskeletal and connective tissue disorders	3 (16.7)	1 (7.1)	1 (5.6)	0
Back pain	3 (16.7)	1 (7.1)	0	0
Metabolism and nutrition disorders	3 (16.7)	0	3 (16.7)	3 (33.3)
Hypercholesterolemia	3 (16.7)	0	1 (5.6)	1 (11.1)
Vascular disorders	1 (5.6)	0	6 (33.3)	0
Hot flush	1 (5.6)	0	5 (27.8)	0

MDE multiple-dose escalation, *N* number of subjects in the intent-to-treat population, *n* number of subjects with adverse events, *SDE* single-dose escalation

laboratory abnormalities were either Grade 1 or 2 in severity. The most frequent TEAEs (≥15%) in subjects on JNJ-53718678, compared with placebo, included hot flush (27.8 vs. 0%) and dysgeusia (16.7 vs. 0%). Hot flush was the only most frequent TEAE assessed by the investigator to be at least possibly related to JNJ-53718678. There were no consistent or clinically relevant changes over time in laboratory safety values, ECGs, or vital signs.

4 Discussion

In this first-in-human study, a double-blind design with consecutive escalating doses was employed to explore the PK profile and determine the safety and tolerability of JNJ-53718678 in healthy adult subjects after single and multiple (for 8 days) dosing. In addition, the food effect on a

single dose of 250 mg (dose proven safe under fasted conditions) of JNJ-53718678 was investigated.

There was a dose-proportional increase in C_{max} with increasing JNJ-53718678 doses from 25 to 1000 mg, while the increase in AUC_{∞} was more than dose proportional in the same dose range. A dose-proportional increase was also observed in C_{max} and AUC_{24h} on days 1 and 8 in the MDE groups with an increase in dose from 250 mg q24h to 500 mg q24h, indicating linear absorption characteristics of JNJ-53718678. The inter-subject variability was high (11.0–123.8%) in the SDE groups and moderate to high (12.1–66.8% on day 1 and 15.4–180.0% on day 8) in the MDE groups.

The mean exposure (AUC_{∞}) of JNJ-53718678 in fed subjects was only 7% lower compared with the fasted subjects despite a 35% decrease in mean C_{max} at the same dose (250 mg), suggesting that JNJ-53718678 can be administered irrespective of food intake. This food effect was adequately described by two separate Ka. Furthermore, the model showed good precision on absorption parameters and acceptable between-subject variability. The model-predicted AUC (approximately 1.5%) and peak concentrations (approximately 13.0%) also decreased under fed conditions. This is similar to the results of the non-compartmental analysis, where a decrease of 35% in C_{max} was reported. Because this difference in C_{max} and AUC under fasted and fed conditions is small, compared with the estimated variability (%CV 18–180%) in MDE groups, it can be concluded that the influence of food intake prior to JNJ-53718678 administration on the absorption of JNJ-53718678 is not clinically relevant. The decreases in C_{max} and a later T_{max} are reflective of delayed gastric emptying in the presence of food [15].

In the MDE groups, steady-state conditions were reached on day 2 of treatment across all dosing groups. The mean C_{trough} values for the 250 mg q12h group were slightly higher than the 500 mg q24h group on all days from days 2 to 8 (Online Resource 6). C_{trough} levels did not change after the second dose, thus steady state was approximated after the second day. A comparison of these C_{trough} values to the in vitro minimum effective concentrations for antiviral effects may help decide between a once- or twice-daily dosing regimen for JNJ-53718678.

The dependence of total clearance (CL) on JNJ-53718678 plasma concentrations was assessed using population estimates of the linear CL and the nonlinear CL components. At JNJ-53718678 plasma concentrations of <589 μg/L, nonlinear CL was the dominant component of total CL; at concentrations >2000 μg/L, linear CL was the dominant elimination pathway. At concentrations ~589 μg/L, both components of total CL contributed equally to the elimination (Fig. 6). Once the contribution of the different elimination pathways of JNJ-53718678 to total CL are quantified, the model could be further optimized to include more physiologically based population modeling and simulations. The minor influence of the non-linear clearance is shown in Online Resources 4 and 5. The difference in CL/*F* of JNJ-678, a 3A4 substrate, between the lowest and highest doses may be owing to partial saturation of 3A4. Additionally, given that JNJ-678 is a P-glycoprotein substrate, saturation of P-glycoprotein in the gut or in the liver at high doses may have increased the fraction

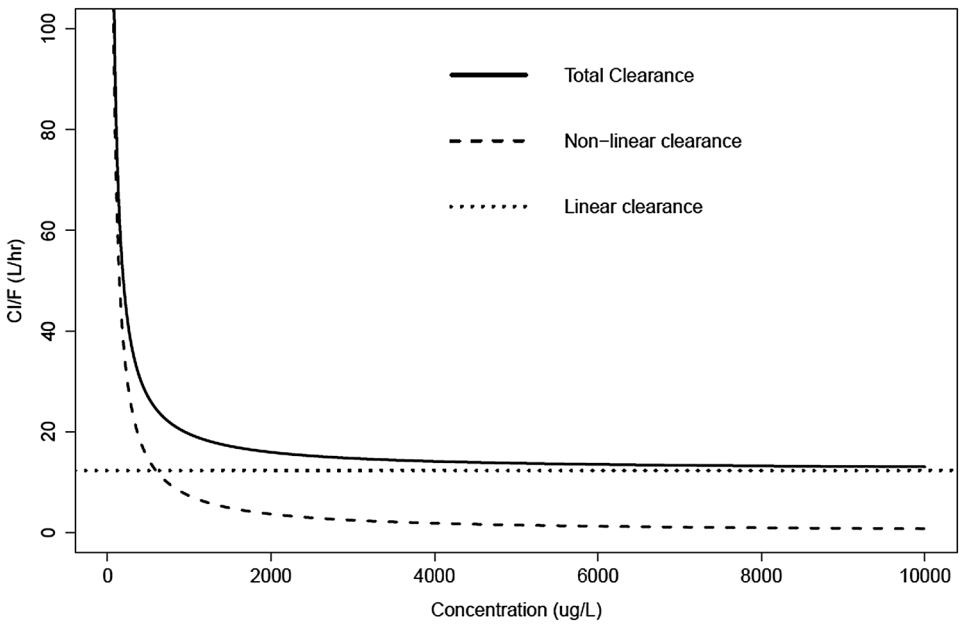

Fig. 6 Relationship between clearance and increasing plasma concentrations using population estimates. *Cl/F* apparent clearance

absorbed and decreased the contribution of biliary CL to the total CL, respectively.

Considering that the mean baseline-corrected concentrations of 4β-hydroxycholesterol were higher for the 250 mg q12h compared with the 500 mg q24h dosing regimen on day 8, it may be concluded that the higher CYP3A4 induction after 250 mg twice daily compared with 500 mg once daily is associated with the relatively higher trough concentrations of JNJ-53718678 at 250 mg twice daily. An in-house drug-drug interaction study (data on file, EudraCT 2014-0022-16) of JNJ-53718678 with midazolam suggested that JNJ-53718678 is a mild inducer and inhibitor of CYP3A4 and both effects counter each other after repeated dosing. This may explain the apparent absence of CYP3A4 auto-induction, as reflected by the increased JNJ-53718678 AUC_{24h} (all three repeated-dosing regimens) after repeated dosing, despite the increased CYP3A4 activity. Additionally, alternate metabolism pathways for JNJ-53718678 (data on file) make JNJ-53718678 less sensitive to changes in CYP3A4 capacity compared with midazolam.

No apparent relationship was observed between the incidences of AEs, (non-)graded laboratory abnormalities, abnormalities in vital sign parameters, or ECG abnormalities and the dose and/or dose regimen of JNJ-53718678 across all dose groups of the study. All AEs were of Grade 1, or exceptionally of Grade 2 and transiently present.

5 Conclusion

We developed a population PK model to describe JNJ-53718678 plasma concentrations after oral administration in healthy subjects. The current population PK model was used, with the inclusion of maturation of the elimination pathways involved, and the implementation of allometric scaling factors to simulate concentration-time profiles under different dosing strategies to match exposure across subjects of different age groups. This will facilitate future studies of this compound and can be employed in additional pharmacokinetic-pharmacodynamic analysis for safety and efficacy.

Compliance with Ethical Standards

Funding This study was funded by Janssen Pharmaceutica NV, Belgium. Dr. Siddharth Mukherjee, Trilogy Writing and Consulting GmbH, Frankfurt, Germany provided medical writing and editorial assistance and this was funded by Janssen Pharmaceutica NV, Belgium.

Conflict of interest At the time of performing the trial, all authors were employees and shareholders of Janssen Pharmaceutica NV, Belgium.

Ethics approval All procedures performed in studies involving human participants were in accordance with the ethical standards of the institutional and/or national research committee and with the 1964 Helsinki Declaration and its later amendments or comparable ethical standards.

Consent to participate Informed consent was obtained from all subjects included in the study.

References

1. Enders G. Chapter 59. Paramyxoviruses. In: Baron S, editor. Medical microbiology. 4th ed. Galveston, Tex: University of Texas Medical Branch at Galveston; 1996.
2. Mazur NI, Martinón-Torres F, Baraldi E, in collaboration with Respiratory Syncytial Virus Network (ReSViNET), et al. Lower respiratory tract infection caused by respiratory syncytial virus: current management and new therapeutics. Lancet. Respir Med. 2015;3:888–900.
3. Nair H, Nokes JD, Gessner BD, et al. Global burden of acute lower respiratory infections due to respiratory syncytial virus in young children: a systematic review and meta-analysis. Lancet. 2010;375:1545–55.
4. National Center for Immunization and Respiratory Diseases (NCIRD), Division of Viral Diseases. 2014. Available from: http://www.cdc.gov/rsv/about/index.html. Accessed 15 Mar 2016.
5. Paes BA, Mitchell I, Banerji A, et al. A decade of respiratory syncytial virus epidemiology and prophylaxis: translating evidence into everyday clinical practice. Can Respir J. 2011;18:e10–9.
6. Falsey AR, Hennessey PA, Formica MA, et al. Respiratory syncytial virus infection in the elderly and high-risk adults. N Engl J Med. 2005;352:1749–59.
7. Bagga B, Woods CW, Veldman TH, et al. Comparing influenza and RSV viral and disease dynamics in experimentally infected adults predicts clinical effectiveness of RSV antivirals. Antivir Ther. 2013;18:785–91.
8. McLellan JS, Ray WC, Peeples ME. Structure and function of RSV surface glycoproteins. Curr Top Microbiol Immunol. 2013;372:83–104.
9. Roymans D, Rigaux P, Kwanten L, et al. Discovery of JNJ-53718678, a potent inhibitor of RSV. 9th International Respiratory Syncytial Virus Symposium: Cape Town; 9–13 Nov 2014.
10. Ackermann M, Alnajjar S, Larios-Mora A, et al. Therapeutic efficacy of JNJ-53718678, a RSV fusion inhibitor, in neonatal lambs. 10th International Respiratory Syncytial Virus Symposium; Patagonia; 28 Sept–1 Oct 2016.
11. Lindbom L, Pihlgren P, Jonsson EN. PsN-Toolkit: a collection of computer intensive statistical methods for non-linear mixed effect modeling using NONMEM. Comput Methods Programs Biomed. 2005;79(3):241–57.
12. Bergstrand M, Hooker AC, Wallin JE, Karlsson MO. Prediction-corrected visual predictive checks for diagnosing nonlinear mixed-effects models. AAPS J. 2011;13(2):143–51.
13. Björkhem-Bergman L, Bäckström T, Nylén H, et al. Comparison of endogenous 4β-hydroxycholesterol with midazolam as markers for CYP3A4 induction by rifampicin. Drug Metab Dispos. 2013;41(8):1488–93.
14. WHO Toxicity Grading Scale for determining the severity of adverse events. In: ICTDR investigator manual: monitoring and reporting of adverse events. February 2003, p. 45. Available from: http://www.icssc.org/Documents/Resources/ICTDR_AE_Manual_February_6_2003_final.pdf. Accessed 2 Mar 2016.
15. Dressman JB, Berardi RR, Dermentzoglou LC, et al. Upper gastrointestinal (GI) pH in young, healthy men and women. Pharm Res. 1990;7(7):756–61.